Synthesis of adjustable spherical four-link mechanisms for approximate multi-path generation

Prasad Vilas Chanekar*, Michael Angelo Amith Fenelon†, Ashitava Ghosal‡

Abstract

An optimization based method is presented for the synthesis of adjustable spherical four-link crank-rocker mechanisms for approximate multi-path generation. The synthesis is done in two stages, first the driving dyad of the spherical mechanism is determined and then the remaining parameters are determined. The method uses a least squares based plane fitting procedure and this result in less number of design variables for optimization than existing approaches. Two numerical examples, including one dealing with generating two different trajectories of a flapping wing micro air vehicle, are presented to demonstrate the effectiveness of the proposed synthesis method.

Keywords: Approximate synthesis, Adjustable spherical four-link mechanism, Multi-path generation, Optimization, Least-squares based plane fitting.

1 Introduction

In spherical mechanisms, the motion all links as well as the coupler path traced by the mechanism lie on the surface of a sphere and, at any moment, each link of the mechanisms is part of a great circle on the sphere. In this paper, we deal with the simplest spherical mechanism with four links and revolute (R) joints (also known in literature as a 4R-spherical mechanism) with all R joint axes intersecting at the centre of the sphere [1, 2]. Spherical mechanisms have a wide variety of applications such as spherical wrists [3], surgical robots [4], flapping- wing micro air-vehicle [5], grippers [6], in the swiveling fans [7], camera orienting device [8] ("Agile Eye") and space applications [9]. In all these applications, orientation of an object is the principle requirement, and instead of using complex multi-degree-of-freedom robots, it is often possible to use a single degree-of-freedom spherical mechanism to perform the orientation task.

Path generation is a classical problem in spherical four-link kinematics. It consists of designing for linkage parameters such that a given point of the mechanism, usually the coupler point, follows a prescribed path [1, 10]. There are two types of path generation problems namely, point-to-point path generation and continuous path generation. In point-to-point path generation the coupler path is specified by small number of points and the coupler point is made to *exactly* pass through all of them. For a spherical four-link mechanism the coupler point can exactly pass through nine points on the surface of the sphere [11]. In continuous path generation, the coupler path is specified by large number of points (much more than nine) and the task is to design the mechanism such

*Graduate Student, Dept. of Mechanical Engg., IISc Bangalore, Email: prasadvc2007@gmail.com

†Scientist, Institute for Robotics and Intelligent Systems, Bangalore, Email: amith.fenelon@gmail.com

‡Corresponding author, Dept. of Mechanical Engg., IISc Bangalore, Email: asitava@mecheng.iisc.ernet.in, Tel. +91 80 2293 2956

that the path traced by the coupler point *approximately* passes through all of them. Spherical path generation is a non-linear design problem which is generally difficult to solve. In this paper, we convert the non-linear design problem into a simpler optimization problem and solve using appropriate numerical techniques.

Compared to the extensive work done in synthesis and design of planar mechanisms, a more modest amount of work has been done in design of spherical mechanism for point-to-point and continuous path generation. The design of 4R-spherical mechanisms using instantaneous screw axes (ISAs) and curve matching techniques are mentioned in the work by Sodhi and co-workers [12, 13]. Synthesis of 4R-spherical path generators using the pole method was done by Tong and Chiang [14]. Spherical four-link mechanisms for finite positions are synthesized by combining traditional precision theory with modern approximate position synthesis in work by Bodduluri and McCarthy [15]. Computer aided design software for 4R-spherical mechanism design based on Burmester's theory is described in Ruth and McCarthy [16]. Four-link path generators were synthesized using method based on numerical continuation [17] and constrained least square optimization [18]. A triangular nomogram for symmetrical coupler curves generated by spherical four-link crank-rocker mechanisms with special dimensions was presented in the work by Lu [19]. The harmonic properties of coupler curves have been used to prepare an atlas of spherical four-link generators to aid mechanism design [20, 21] and optimization based on differential evolution algorithm has been used for synthesis spherical 4R mechanism [22]. A computer aided methodology for the manufacture of spherical mechanisms is discussed in reference [7] and a review of recent advances and trends in spherical mechanisms research are listed in the work by Liu and Yang [23].

Adjustable mechanisms are a class of mechanisms in which different paths (orientations in case of spherical mechanisms) can be achieved by changing one of the mechanism parameters [24]. Very little work on adjustable spherical mechanism synthesis is available in literature. Adjustable spherical 4R linkages with fixed ground pivots and adjustable lengths for input and output links for five position synthesis by the use of Burmester curves was proposed by Hong and Erdman [25]. The method can be extended to six position synthesis with adjustable ground pivot locations. A method based on plane-to-sphere and sphere-to-plane projections was developed by Lee [24]. Lee et al. [26] describes a least squares minimization technique to synthesize two phase adjustable spherical mechanisms for approximate path generation and path generation using adjustable crank-lengths of spherical four-link mechanisms is suggested in [27]. A new chaos fractal based algorithm for path synthesis of adjustable spherical 4R mechanism is presented in reference [28].

The synthesis of four-link adjustable mechanisms has been done in the planar domain by an optimization based two stage process [29]. The first stage determines the driving dyad and the second stage determines the driven dyad. The sequential quadratic programming (SQP) algorithm [30] is used to search for the optimal design variables which are the Cartesian coordinates of the joints. In a more recent work, an efficient two stage optimization process based on circle fitting has been proposed [31]. A similar kind of optimization based approach is suggested for synthesis of spherical 4R mechanism in this work. In this paper, a least squares plane fitting based formulation is suggested. The paper deals with single adjustment, either on the driven or driving side, in one of the spherical 4R mechanism parameters (except the crank pivot) to approximately generate multiple paths. This paper also presents a novel technique to indirectly calculate some of the mechanism parameters thereby reducing the number of variables required for optimization. The SQP optimization algorithm involving minimum number of optimization variables is used in the formulation of objective function for each type of adjustment. To the best of our knowledge this work presents the first attempt in optimal design of adjustable spherical four-link mechanisms for approximate multi-path generation. The proposed formulation is illustrated with the help of two examples – one example deals with the generation of an oval and '8' shaped path similar to the flapping motion of a bird wing in forward motion and in the hovering mode.

The paper is organized as follows: In section 2, for the sake of completeness, all the parameters associated with the spherical four-link mechanism are defined and we present a procedure for

calculating the necessary parameters. In section 3, the mechanism synthesis problem needed is presented and the rationale behind the selection of the adjustment method is presented. In section 4, examples illustrating our approach are presented and in section 5, conclusions are presented.

2 A spherical four-link mechanism

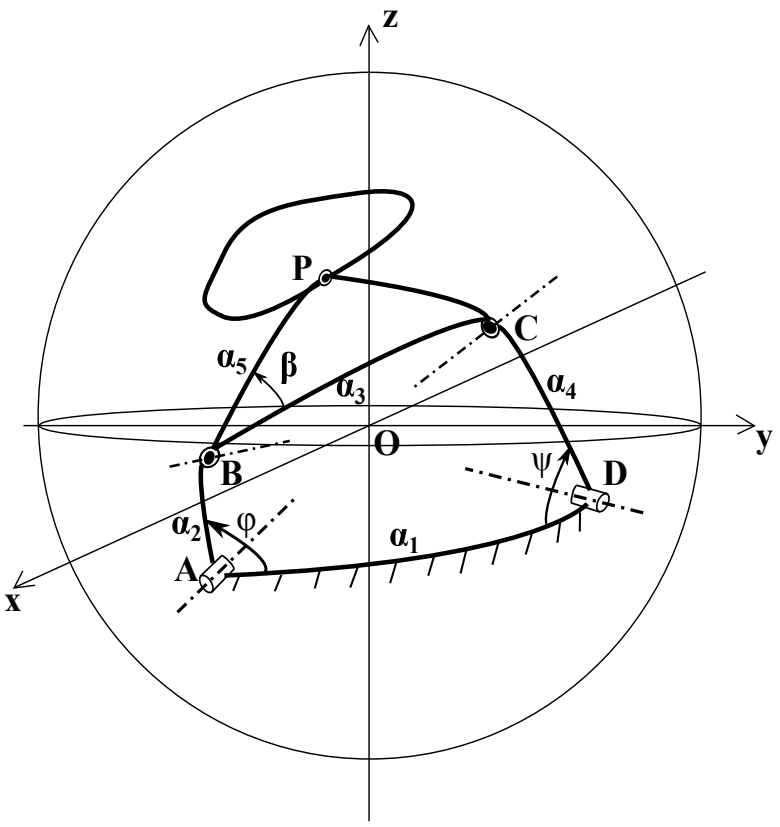

Figure 1: Schematic of a spherical 4R mechanism

The four-link spherical mechanism $OABCDP$ with its parameters is shown on figure 1. The mechanism has four revolute joints at A, B, C and D with their axes intersecting at the center of the sphere O. The links of the mechanism are the arcs of great circles of the sphere and the spherical link length is the arc-length measured on the great circle between two ends of the link. For a sphere of unit radius, the link length is same as the central angle subtended at O by the arc on the great circle. In figure 1, AD is the base or fixed link, AB is the crank, BC is the coupler link, CD is the rocker link, BP is the α_5-link and P is the coupler point. In spherical domain all angles are dihedral angles, i.e., angles are measured between two great circle planes. The line of intersection of the two circular planes is the axis about which the angle is measured. The variable β is the coupler angle measured about the axis OB in counter-clockwise direction, ABP is the driving dyad and DCB is the driven dyad. The crank angle ϕ and the rocker angle ψ are measured with respect to the base link AD and about OA and OD, respectively. The center of the sphere is $O\,(0,0,0)$ and $x^2+y^2+z^2=1$ is the equation of the sphere. The symbols $A\,(x_A,y_A,z_A)$, α_2 and α_5 denote the driving side parameters and $D\,(x_D,y_D,z_D)$, α_3, α_4 and β are the driven side parameters. The vector $\boldsymbol{r}_p=\overrightarrow{\boldsymbol{OP}}=\begin{bmatrix}r_{P_x} & r_{P_y} & r_{P_z}\end{bmatrix}^T$ is the position vector of point P, and $[T_\delta^{\boldsymbol{n}}]$ is

the rotation matrix, $\boldsymbol{n} = [n_x \quad n_y \quad n_z]^T$ is an unit vector corresponding to the axis of rotation and δ is the angle of rotation about $\boldsymbol{n}$ in counter-clockwise direction. From [32], the rotation matrix is defined as,

$$[T_\delta^{\boldsymbol{n}}] = \begin{bmatrix} \cos\delta + n_x^2(1-\cos\delta) & n_x n_y(1-\cos\delta) - n_z\sin\delta & n_x n_z(1-\cos\delta) + n_y\sin\delta \\ n_x n_y(1-\cos\delta) + n_z\sin\delta & \cos\delta + n_y^2(1-\cos\delta) & n_y n_z(1-\cos\delta) - n_x\sin\delta \\ n_x n_z(1-\cos\delta) - n_y\sin\delta & n_y n_z(1-\cos\delta) + n_x\sin\delta & \cos\delta + n_z^2(1-\cos\delta) \end{bmatrix} \quad (1)$$

The driving crank pivot $A(x_A, y_A, z_A)$ remains unchanged in our approach. The desired paths are represented by 50 to 100[1] points and if lesser number of points are prescribed then spline interpolation can be used to generate additional points on the path. The super-script of the mechanism parameter indicates the path to which it belongs.

In planar domain, the workspace of the end-point of a dyad lies between two concentric circles [32]. Drawing parallels from the planar case, the workspace of the end-point of a spherical dyad lies between two coaxial spherical small circles[2], i.e., spatial circles about the same axis. All the coupler paths generated by the mechanism must lie inside the boundaries of the workspace of the dyad where the boundaries are dependent on the dimensions of the driving dyad ABP. The dimensions of the driving dyad are chosen such that the workspace boundaries are tangential to the given coupler paths. It can be seen that the small circles with spherical radii[3] α_{max} and α_{min} form the boundary of the workspace of the driving dyad. Similar to the planar case [31], for a spherical four-link mechanism the location of the pivot A on the sphere is outside the coupler path if $\alpha_5 > \alpha_2$ and inside the coupler path if $\alpha_5 < \alpha_2$. This fact helps in choosing fixed pivot A.

For N given points $P_i(x_{P_i}, y_{P_i}, z_{P_i}), i = 1, 2, \ldots, N$, on each coupler path, we define

$$\begin{aligned} \alpha_{max} &= \max\{\alpha_{P_1}, \alpha_{P_2}, \ldots, \alpha_{P_N}\} \\ \alpha_{min} &= \min\{\alpha_{P_1}, \alpha_{P_2}, \ldots, \alpha_{P_N}\} \end{aligned} \quad (2)$$

where, $\alpha_{P_i} = \cos^{-1}(\boldsymbol{r}_{P_i} \cdot \boldsymbol{r}_A)$ for $i = 1, 2, \ldots, N$ and

$$\begin{aligned} &\boldsymbol{r}_A = [x_A \quad y_A \quad z_A]^T \\ &x_A = \cos\tau\sin\kappa, \quad y_A = \sin\tau\sin\kappa, \quad z_A = \cos\kappa \\ &\kappa \in [0, \pi] \quad \text{and} \quad \tau \in [0, 2\pi] \end{aligned} \quad (3)$$

where (τ, κ) are the spherical polar coordinates of A. The quantity κ is the polar angle with respect to the $+Z$-axis and τ is the azimuthal angle in the XY-plane with respect to the $+X$-axis. We are designing for $0 < \alpha_{max} < \pi$. The quantities α_2 and α_5 are chosen such that,

$$\begin{aligned} \alpha_{max} &= \alpha_2 + \alpha_5 \\ \alpha_{min} &= |\alpha_5 - \alpha_2| \end{aligned} \quad (4)$$

For each P_i of the coupler path there is a corresponding B_i and θ_i. The points B_i represent the two configurations of the crank to reach P_i and θ_i is the angle between AB_i and $AP_{\max}$ where $P_{\max}$

[1]The proposed methods also work for a lesser number of points but larger number of points help in increasing the accuracy of plane fitting used in **Stage II** of the design process. After extensive simulations we have found that 50-100 points give sufficient accuracy.

[2]A spherical small circle is any circle other than the great circle on the surface of the sphere.

[3]The spherical radius is the angle between $\overrightarrow{OA}$ and $\overrightarrow{OQ}$ with Q being any point on the small circle.

is the coupler point on the spherical surface farthest from pivot A (see figure 2). There are two possible values of θ_i, as shown in figure 2, and these can be computed as,

$$\theta_i = \alpha_i \pm \gamma_i \tag{5}$$

where γ_i determine the two configurations of the crank for a particular P_i. It should be noted that the angles θ and ϕ (see figure 1) are two different quantities although they are related to the crank. As shown in figure 1, the angle ϕ is between the crank and the fixed link whereas angle θ is between the crank and $AP_{\max}$. The angles are also with respect to two different planes – the angle ϕ is with respect to the great circular plane containing the fixed link AD and centre of the sphere whereas θ_i is with respect to fixed pivot A, the sphere centre O and the coupler point P farthest from A.

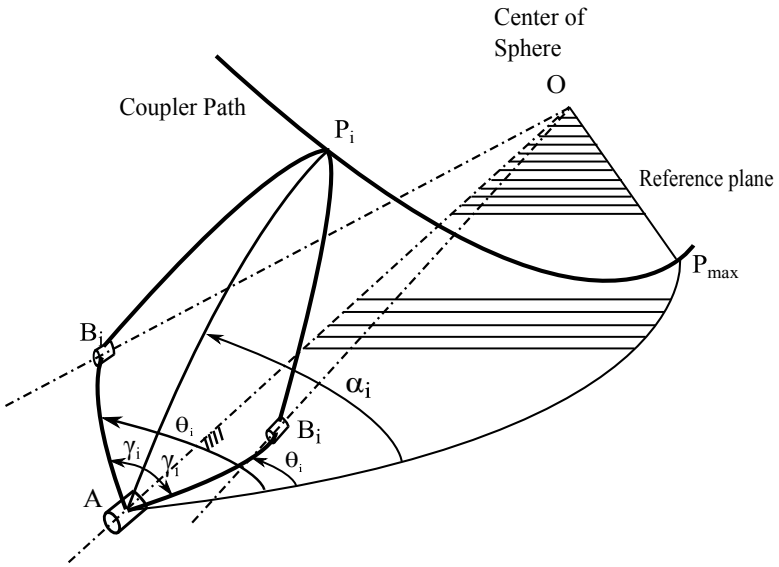

Figure 2: Crank angle and a spherical dyad

From the above, we can write the following:

$$\begin{aligned}
\boldsymbol{n}_{max} &= \frac{\boldsymbol{r}_A \times \boldsymbol{r}_{P_{\max}}}{||\boldsymbol{r}_A \times \boldsymbol{r}_{P_{\max}}||} \\
\boldsymbol{n}_{P_i} &= \frac{\boldsymbol{r}_A \times \boldsymbol{r}_{P_i}}{||\boldsymbol{r}_A \times \boldsymbol{r}_{P_i}||} \\
\alpha_i &= \cos^{-1}\left(\boldsymbol{n}_{max} \cdot \boldsymbol{n}_{P_i}\right) \\
\gamma_i &= \cos^{-1}\left(\frac{\cos\alpha_5 - \cos\alpha_2 \cos\alpha_{P_i}}{\sin\alpha_2 \sin\alpha_{P_i}}\right) \\
0 \leq (\alpha_i, \theta_i) &\leq 2\pi \quad \text{and} \quad 0 \leq \gamma_i \leq \pi
\end{aligned}$$

A notable fact here is that in one crank rotation, the coupler point P crosses α_{max} and α_{min} once, thus dividing the rotation into two parts. The sign of γ_i in one α_{max} to α_{min} part is opposite to that of the remaining α_{min} to α_{max} part. Thus each given coupler path will have two sets of θ_i and if the direction of rotation is not specified, appropriate θ_i must be chosen. For the reference plane, $\alpha_{P_i} = \alpha_{max}$, which means that A, B and $P_{\max}$ lie in the same great circle. For the path point $P_{\max}$,

the corresponding $\theta_i = 0$ and position vector of B is $r_{B_{max}}$. Using equation (1), we find B_i from

$$\begin{aligned} \boldsymbol{r}_{B_{max}} &= \left[T_{\alpha_2}^{\boldsymbol{n}_{max}}\right] \begin{bmatrix} x_A & y_A & z_A \end{bmatrix}^T \\ \boldsymbol{r}_{B_i} &= \left[T_{\theta_i}^{\boldsymbol{r}_A}\right] \boldsymbol{r}_{B_{max}} \end{aligned} \tag{6}$$

The position of the corresponding point C_i is,

$$\begin{aligned} \boldsymbol{n}_{C_i} &= \frac{\boldsymbol{r}_{B_i} \times \boldsymbol{r}_{P_i}}{||\boldsymbol{r}_{B_i} \times \boldsymbol{r}_{P_i}||} \\ \boldsymbol{r}_{C_i} &= \left[T_{-\beta}^{\boldsymbol{r}_{B_i}}\right] \left[T_{\alpha_3}^{\boldsymbol{n}_{C_i}}\right] \boldsymbol{r}_{B_i} \end{aligned} \tag{7}$$

With the above definitions and kinematic equations, we next formulate the adjustable mechanism synthesis problem.

3 The spherical mechanism synthesis problem

The synthesis problem is to find the dimensions of the adjustable mechanism such that the given coupler paths can be traced as closely as possible. The spherical four-link adjustable mechanism can be classified based on the adjustment parameter as follows:
a) Adjustable crank mechanism, b) Adjustable α_5-link mechanism, c) Adjustable rocker pivot mechanism, d) Adjustable rocker link mechanism, and e) Adjustable coupler link mechanism.

The design process is divided into stages. In **Stage I** all the possible locations of crank pivot A are determined. The **Stage II** is used to complete the synthesis of the mechanism using the output of **Stage I**. In the following, the objective functions are derived for $\alpha_5 > \alpha_2$. The formulations are also valid for $\alpha_5 < \alpha_2$ with equation (4) as $\alpha_{min} = \alpha_2 - \alpha_5$.

3.1 Stage I: Computation of possible locations of A

Since the number of path points are much more than 9, optimization is used to determine the possible locations of crank pivot A. Using the facts stated above regarding pivot A, the optimization problem for the computation of pivot A can be set for each type of adjustable mechanism.

Adjustable crank length mechanism
The crank length α_2 is changed with all other mechanism parameters remaining the same to get multiple paths. The change in the crank length α_2 causes a change in the size of the workspace boundaries as well as the size of the coupler path on the surface of the sphere but the shape of the path remains almost the same. For the $\alpha_5 > \alpha_2$ type mechanisms, consider two coupler paths denoted by superscripts '1' and '2'. Using equation (2), for $\alpha_2^2 > \alpha_2^1$, $\alpha_{max}^2 > \alpha_{max}^1$ and $\alpha_{min}^2 < \alpha_{min}^1$, the first workspace is completely enclosed by the second workspace and the bigger coupler path completely encloses the smaller coupler path[4]. For the case $\alpha_5 > \alpha_2$, using equations (2), (3) and

[4]For $\alpha_5 < \alpha_2$, the same behaviour is observed except $\alpha_{min}^2 > \alpha_{min}^1$.

(4), for the i^{th} path, we can write

$$\begin{aligned}
\alpha_5^i &= \frac{\alpha_{max}^i + \alpha_{min}^i}{2} \\
\alpha_2^i &= \frac{\alpha_{max}^i - \alpha_{min}^i}{2} \\
\alpha_5 &= \max\left\{\alpha_5^1, \alpha_5^2, \ldots, \alpha_5^m\right\} \\
\alpha_{21}^i &= \alpha_{max}^i - \alpha_5 \\
\alpha_{22}^i &= \alpha_5 - \alpha_{min}^i
\end{aligned} \tag{8}$$

where m is the total number of given paths to be traced by the mechanism.

Since link length α_5 is not changed during adjustment, we must have,

$$\alpha_5^i - \alpha_5^j = 0 \quad \forall i \neq j \quad \text{and} \quad i, j \in \{1, 2, \ldots, m\}$$

For each individual i^{th} coupler path the corresponding crank length remains fixed. Hence we can write,

$$\alpha_2^i - \alpha_{21}^i = 0 \quad \text{and} \quad \alpha_2^i - \alpha_{22}^i = 0$$

From above the optimization problem with i, j, and k indices representing different coupler paths can be written as[5],

$$\begin{aligned}
&Minimize \\
&S(\kappa, \tau) = \sum_{i=1}^{m-1} \sum_{j=i+1}^{m} \left(\alpha_5^i - \alpha_5^j\right)^2 + \sum_{k=1}^{m} \left(\alpha_2^k - \alpha_{21}^k\right)^2
\end{aligned} \tag{9}$$

Subject to the following constraints,

Constraint 1: Search space restriction for κ and τ

$$\kappa \in [0, \pi] \quad \text{and} \quad \tau \in [0, 2\pi] \tag{10}$$

Constraint 2: The crank angle should always increase or decrease as P advances along the coupler path. The conditions for the counter-clockwise and clockwise rotation of the crank respectively are,

$$\begin{aligned}
&\theta_{(q+1)}^i - \theta_q^i > 0 \\
&\theta_{(q+1)}^i - \theta_q^i < 0 \\
&\text{for} \quad q = 1, 2, \ldots, N-1
\end{aligned} \tag{11}$$

where, N is the total number of points P_q^i on the given i^{th} coupler path and each θ_q is calculated using equation (3). It maybe noted that one of the conditions in equation (11) also needs to be satisfied.

Constraint 3: The maximum length of the coupler link α_5 must satisfy

$$\alpha_5^i < \alpha_{5max} \tag{12}$$

[5]In the objective function, the term $\left(\alpha_{22}^k - \alpha_2^k\right)^2$ can also be used instead of $\left(\alpha_{21}^k - \alpha_2^k\right)^2$ and the chosen α_{21} (or α_{22}) should be used in subsequent computations.

Adjustable α_5-link length mechanism
The adjustment in the α_5-link length changes the workspace boundary dimensions. For $\alpha_5 > \alpha_2$ type mechanisms, changing α_5 (with $\alpha^2_{max} > \alpha^1_{max}$ and $\alpha^2_{min} > \alpha^1_{min}$ and $\alpha^2_5 > \alpha^1_5$) results in a common space between the original workspace and the workspace after the change[6]. The bigger coupler path does not enclose the smaller coupler path but they may intersect. The size of the coupler path changes but the shape is almost unchanged. From equation (2), we can write

$$\begin{aligned}
\alpha^i_5 &= \frac{\alpha^i_{max} + \alpha^i_{min}}{2} \\
\alpha^i_2 &= \frac{\alpha^i_{max} - \alpha^i_{min}}{2} \\
\alpha_2 &= \max\left\{\alpha^1_2, \alpha^2_2, \ldots, \alpha^m_2\right\} \\
\alpha^i_{51} &= \alpha^i_{max} - \alpha_2 \\
\alpha^i_{52} &= \alpha_2 + \alpha^i_{min}
\end{aligned} \tag{13}$$

where m is the total number of given paths to be traced by the mechanism.

Since link length α_2 remains fixed throughout the adjustment then we must have,

$$\alpha^i_2 - \alpha^j_2 = 0 \quad \forall i \neq j \quad \text{and} \quad i, j \in \{1, 2, \ldots, m\}$$

For each individual i^{th} coupler path the corresponding crank length remains fixed. Hence we can write,

$$\alpha^i_5 - \alpha^i_{51} = 0 \quad \text{and} \quad \alpha^i_5 - \alpha^i_{52} = 0$$

From above the optimization problem with i, j, and k indices representing different coupler paths can be written as[7],

$$\begin{aligned}
&Minimize \\
&S(\kappa, \tau) = \sum_{i=1}^{m-1} \sum_{j=i+1}^{m} \left(\alpha^i_2 - \alpha^j_2\right)^2 + \sum_{k=1}^{m} \left(\alpha^k_5 - \alpha^k_{51}\right)^2
\end{aligned} \tag{14}$$

Subject to the constraints (10), (11) and (12) given above.

Adjustable rocker pivot, rocker length and coupler length mechanisms
All these type of adjustable mechanisms have fixed workspace boundaries and since the driving dyad dimensions remain constant leading, α_{max} and α_{min} are fixed. The design is for $0 \leq \alpha_{max}, \alpha_{min} \leq \pi$ with α_{max} and α_{min} found as in equation (2). The quantities α_{max} and α_{min} also correspond to maximum and minimum Euclidean distances between pivot A and path points P_{max} and P_{min}, respectively. Hence, for the coupler paths belonging to the same workspace we must have

$$\begin{aligned}
&l^i_{max} - l^j_{max} = 0 \quad \text{and} \quad l^i_{min} - l^j_{min} = 0 \quad \text{for} \quad i \neq j \\
&i, j \in \{1, 2, \ldots, m\}
\end{aligned} \tag{15}$$

As mentioned earlier, the workspace of the mechanism is chosen such that all the coupler paths are tangential to the workspace boundaries. The optimization problem for determining the optimal

[6]For $\alpha_5 < \alpha_2$, the same behaviour is observed except $\alpha^2_{min} < \alpha^1_{min}$.

[7]In the objective function, the term $\left(\alpha^k_{52} - \alpha^k_5\right)^2$ can also be used instead of $\left(\alpha^k_{51} - \alpha^k_5\right)^2$ and the chosen α_{51} (or α_{52}) should be used in subsequent computations.

location of crank pivot A with i and j indices representing different coupler paths for this case can be formulated as:

$$\begin{aligned} &Minimize \\ &S(\kappa,\tau) = \sum_{i=1}^{m-1}\sum_{j=i+1}^{m}\left[\left(l^i_{max}-l^j_{max}\right)^2+\left(l^i_{min}-l^j_{min}\right)^2\right] \\ &\text{where}\quad l^i_k = ||\boldsymbol{r}_A - \boldsymbol{r}^i_{P_k}||,\quad l^i_{max} = \max\left\{l^i_1, l^i_2, \ldots, l^i_N\right\},\quad l^i_{min} = \min\left\{l^i_1, l^i_2, \ldots, l^i_N\right\} \end{aligned} \tag{16}$$

Subject to the constraints (10), (11) and (12) given earlier.

In the above, P^i_k is the k^{th} path point on the i^{th} coupler path and N denotes the total number of given path points on each coupler path. Once the optimal location of A is determined, the corresponding α_2 and α_5 are computed using equations (2) and (4).

In this work, the optimization is carried out using the SQP [30] algorithm and it is known that SQP converges to a local minimum closest to the initial guess. To obtain other possible minima, we divide the search space of optimization variables (κ,τ) into several sub-intervals and take mid-point of the sub-interval as the starting point of the optimization and we get one optimal solution for each sub-interval. To reduce the number of solutions, all solutions whose objective function value, S, is less than some user defined S_{max} are selected. In this work S_{max} is chosen $\leq 10^{-3}$ for reasonable accuracy. The driving dyads parameters determined in **Stage I** are passed to **Stage II** to determine all the other 4R spherical mechanism parameters.

3.2 Stage II: Synthesis of the complete 4R spherical mechanism

In this stage the complete mechanism is determined using the driving dyads computed in **Stage I**. The central idea of the synthesis is that the locus traced by the point C as the point P moves along the coupler path is an arc on a spatial circle where this spatial circle is a small circle on the surface of the sphere. The intersection of a plane and a sphere is a circle, hence the locus of all the points C is a plane. The minimization objective function formulated for the synthesis purpose is the residual error obtained by *plane fitting* all the points C_i corresponding to coupler path points P_i. The algorithm used for least squares plane fitting is similar to the algorithm used for circle fitting given in [33]. For each of the types mentioned below, the optimization variables are coupler link length α_3 and coupler angle β. The points C_i can be computed using equations (5), (6) and (7) for all adjustments. As in **Stage I**, the optimization is performed using SQP algorithm [30] which converges to a local minimum. Similar to **Stage I**, the search space of optimization variables (α_3,β) is divided into several sub-intervals and the mid-point of each sub-interval is taken as the starting point of optimization.

Adjustable crank and α_5-link length mechanisms
Only the driven dyad is adjusted in these type of mechanisms and since the rocker pivot and rocker length remain fixed, the point C will trace arcs corresponding to each given coupler path on the same spatial circle. This spatial circle can be generated by the intersection of a fixed plane and sphere. The required objective function can be written as,

$$\begin{aligned} &Minimize \\ &f(\alpha_3,\beta) = \sum_{i=1}^{m}\sum_{j=1}^{N}\frac{\left(ax^i_{C_j}+by^i_{C_j}+cz^i_{C_j}+d\right)^2}{a^2+b^2+c^2} \end{aligned} \tag{17}$$

Subject to the following constraints:

Constraint 1:

$$\alpha_2^i < \alpha_3 \leq \alpha_{3max} \tag{18}$$

Constraint 2:

$$-\pi \leq \beta \leq \pi \tag{19}$$

Constraint 3:

$$\alpha_2^i < \alpha_1 \quad \text{and} \quad \alpha_2^i < \alpha_4 \tag{20}$$

Constraint 4: For link CD to be a rocker, the angular sweep of link CD should be less than π radians.

$$\psi_{max} - \psi_{min} < \pi \tag{21}$$

Constraint 5:
Grashof's criterion for crank-rocker type mechanism [1] should be satisfied for each i^{th} path.

The quantity f in (17) represents the error in the least squares plane-fitting of C_i on the plane defined by parameters (a, b, c, d). The least squares fitting algorithm used above is similar to circle fitting algorithm given in [33] where the algebraic fitting or linear problem in [33] is replaced by the equation of a plane, namely $f_1 = ax + by + cz + d$, and the geometric fitting or non-linear least squares problem is replaced by f given in equation (17). The SQP algorithm is used for optimization with the search space divided into several sub-intervals with the mid-point of the each sub-interval used as the starting point of optimization in the corresponding sub-interval. Since from **Stage I**, the crank pivot A and the driving dyad are already known, the remaining parameters are computed using the optimal plane as follows,

$$\begin{aligned} \text{fixed pivot } D &= \left(\frac{a}{\sqrt{a^2+b^2+c^2}}, \frac{b}{\sqrt{a^2+b^2+c^2}}, \frac{c}{\sqrt{a^2+b^2+c^2}} \right) \\ \alpha_4 &= \cos^{-1}\left(\frac{||d||}{a^2+b^2+c^2} \right) \\ \alpha_1 &= \cos^{-1}\left(\boldsymbol{r}_A \cdot \boldsymbol{r}_D \right) \end{aligned} \tag{22}$$

$$\begin{aligned} \text{fixed pivot } D &= \left(\frac{-a}{\sqrt{a^2+b^2+c^2}}, \frac{-b}{\sqrt{a^2+b^2+c^2}}, \frac{-c}{\sqrt{a^2+b^2+c^2}} \right) \\ \alpha_4 &= \pi - \cos^{-1}\left(\frac{||d||}{\sqrt{a^2+b^2+c^2}} \right) \\ \alpha_1 &= \pi - \cos^{-1}\left(\boldsymbol{r}_A \cdot \boldsymbol{r}_D \right) \end{aligned} \tag{23}$$

The link length α_4 calculated in equation (22) will always be in $\left[0, \frac{\pi}{2}\right]$ and α_4 calculated in equation (23) will always be in $\left[\frac{\pi}{2}, \pi\right]$. It should be noted that the assembly mode of the mechanism synthesized in (22) is opposite to that synthesized using (23). The **Stage II** is performed on each driving dyad passed on from **Stage I**. The mechanism having minimum sum of cost functions of **Stage I** and **Stage II**, i.e., $(S + f)_{min}$ is selected. Miscellaneous constraints related to the specific application of the mechanism may also be applied during or after optimization.

Adjustable coupler length mechanism
In this case the coupler length is the adjustable parameter with the driving dyad and crank pivot remaining the same. The rocker point C will trace arc belonging to the same spatial circle like the adjustable crank case. Since the coupler length α_3 is required for the computation of points C for each coupler path, the optimization variables for this case are $(\alpha_1, \alpha_2, \ldots, \alpha_m, \beta)$ unlike the adjustable crank case. Since the formulation of the objective function depends only on the points

C_i the objective function remains same as in (17) and the evaluation procedure for rest of the mechanism parameters as in adjustable crank case. The constraints for the optimization are same as in (19), (21), (18) modified as $\alpha_2 < \alpha_3^i \leq \alpha_{3max}$ and (20) modified as $\alpha_2 < \alpha_1 \quad \text{and} \quad \alpha_2 < \alpha_4$. Additionally Grashof's criterion for crank-rocker type mechanism needs to be satisfied.

Adjustable rocker pivot mechanism
In this type, the rocker pivot D is the adjustment parameter but the rocker length α_4 and all other mechanism parameters remains fixed. The rocker point C will trace different spatial circular arcs with same radius but different axes corresponding to each given coupler path. These arcs will lie in different planes which are at a same perpendicular distance d from the center of the sphere O. The different planes have parameters (a_i, b_i, c_i, d_i) corresponding to the i^{th} coupler path.

$$\frac{||d_i||}{\sqrt{a_i^2 + b_i^2 + c_i^2}} = d$$

Taking positive sign we can write,

$$d_i = d\sqrt{a_i^2 + b_i^2 + c_i^2}$$

Using above fact the objective function, the least squares plane fitting error, can be written as,

$$Minimize: \\ f(\alpha_3, \beta) = \sum_{i=1}^{m}\sum_{j=1}^{N}\left(\frac{a_i x_{C_j^i} + b_i y_{C_j^i} + c_i z_{C_j^i}}{\sqrt{a_i^2 + b_i^2 + c_i^2}} + d\right)^2 \tag{24}$$

Subject to constraints (18), (19), (21), satisfaction of Grashof's criterion and (20) replaced by $\alpha_2 < \alpha_4$ and $\alpha_2 < \alpha_1^i$. The points $C_j^i\left(x_{C_j^i}, y_{C_j^i}, z_{C_j^i}\right)$ are determined using equations (6) and (7).

The plane parameters (a_i, b_i, c_i, d) are required to evaluate the objective function f in (24) during each optimization iteration. To get the plane parameters for each optimization iteration, the optimization problem is converted into a non-linear least squares problem for the corresponding iteration. This non-linear least squares problem is solved using Gauss-Newton method [34] which needs a starting value for the unknowns. The two-step procedure for solving this problem is given as follows:

Step 1: Set of C_j^is for each i^{th} coupler path are individually plane fitted to obtain $(a_{is}, b_{is}, c_{is}, d_{is})$ for each i^{th} coupler path.

Step 2: The non-linear least squares problem stated in equation (24) is formed using (a_i, b_i, c_i, d) as unknown variables is solved using the output of Step 1 given above as starting values. The starting value for each (a_i, b_i, c_i) set is the set (a_{is}, b_{is}, c_{is}) and the starting value for d is $\min\{d_{1s}, d_{2s}, \ldots, d_{ms}\}$ or $\frac{1}{m}\left(\sum_{i=1}^{m} d_{is}\right)$.

After getting the plane parameters, the corresponding D_i, α_1^i and α_4 for the i^{th} coupler path can be computed using (22) or (23).

Adjustable rocker length mechanism
In this case, the rocker length α_4 is the adjustment parameter but the rocker pivot D and all other

mechanism parameters remain fixed. The rocker point C will trace different spatial circular arcs with same axes but different radii corresponding to each given coupler path. These arcs will lie in different parallel planes with different perpendicular distance from the center of the sphere O. The different planes have parameters (a, b, c, d_i) corresponding to the i^{th} coupler path. The objective function for the optimization in this case can be written as,

$$\begin{aligned} &Minimize: \\ &f(\alpha_3, \beta) = \sum_{i=1}^{m} \sum_{j=1}^{N} \left(\frac{a x_{C_j^i} + b y_{C_j^i} + c z_{C_j^i}}{\sqrt{a^2 + b^2 + c^2}} + d_i \right)^2 \end{aligned} \tag{25}$$

Subject to constraints (18), (19), and (21), satisfaction of Grashof's criterion and (20) replaced by $\alpha_2 < \alpha_4^i$ and $\alpha_2 < \alpha_1$.

Similar to adjustable rocker pivot formulation, the plane parameters (a, b, c, d_i) are required to evaluate the objective function f in (25) during each optimization iteration. To get the plane parameters for each optimization iteration, the optimization problem is converted into a non-linear least squares problem for the corresponding iteration. Similar to earlier case, the non-linear least squares problem is solved using the Gauss-Newton method [34] which needs a starting value for the unknowns. The two-step procedure for solving this problem is as follows:

Step 1: Set of C_j^is for each i^{th} coupler path are individually plane fitted to obtain $(a_{is}, b_{is}, c_{is}, d_{is})$ for each i^{th} coupler path.

Step 2: The non-linear least squares problem stated in equation (25) is formed using (a, b, c, d_i) as unknown variables and is solved using the output of Step 1 given above as starting values. The starting value for each (a, b, c, d_i) set is the set (a_s, b_s, c_s, d_{is}), where

$$a_s = \frac{1}{m} \left(\sum_{i=1}^{m} a_{is} \right), \quad b_s = \frac{1}{m} \left(\sum_{i=1}^{m} b_{is} \right), \quad c_s = \frac{1}{m} \left(\sum_{i=1}^{m} c_{is} \right)$$

After getting the plane parameters, the corresponding D_i, α_1^i and α_4 for the i^{th} coupler path can be computed using (22) or (23).

For each of 4R spherical mechanism type given above, the mechanism with minimum $(S + f)$ and satisfying all constraints given above must be selected. The qualitative study of variation of planar four-bar coupler paths with changes in different mechanism parameters has been done in [27, 35, 36]. Parallels can be drawn from this study to gain an insight of qualitative changes in spherical 4R coupler paths with respect to each adjustment parameter. The quantitative effect of the adjustment can be accounted by computing the error in the given and generated coupler paths. The error can be calculated as below,

3.3 Error computation

The error computation assists us in choosing the adjustment type when we cannot ascertain the choice qualitatively. With respect to figure 1, the input-output equation [37] for spherical four-link mechanism is given as,

$$\psi_j = 2 \tan^{-1} \left(\frac{-Q \pm \sqrt{Q^2 + R^2 - S^2}}{S - R} \right) \tag{26}$$

where,

$$
\begin{aligned}
Q &= \sin\alpha_2 \sin\alpha_4 \sin\phi_j \\
R &= \cos\alpha_2 \sin\alpha_4 \sin\alpha_1 - \sin\alpha_2 \sin\alpha_4 \cos\alpha_1 \cos\phi_j \\
S &= \cos\alpha_2 \cos\alpha_4 \cos\alpha_1 + \sin\alpha_2 \cos\alpha_4 \sin\alpha_1 \cos\phi_j - \cos\alpha_3
\end{aligned}
$$

The position vector of point B, $\boldsymbol{r}_{B_j}$ and C, $\boldsymbol{r}_{C_j}$ are given as,

$$
\begin{aligned}
&\boldsymbol{r}_{B_{base}} = \left[T_{\alpha_2}^{\boldsymbol{n}_{base}}\right] \boldsymbol{r}_A \\
&\boldsymbol{r}_{B_j} = \left[T_{\phi_j}^{\boldsymbol{r}_A}\right] \boldsymbol{r}_{B_{base}} \\
&\boldsymbol{r}_{C_{base}} = \left[T_{-\alpha_4}^{\boldsymbol{n}_{base}}\right] \boldsymbol{r}_D \\
&\boldsymbol{r}_{C_j} = \left[T_{-\psi_j}^{\boldsymbol{r}_D}\right] \boldsymbol{r}_{C_{base}} \\
&\text{where} \quad \boldsymbol{n}_{base} = \frac{\boldsymbol{r}_A \times \boldsymbol{r}_D}{||\boldsymbol{r}_A \times \boldsymbol{r}_D||}
\end{aligned}
\tag{27}
$$

The position vector of desired path P_j is $\boldsymbol{r}_{CP_j}$ given by 100 points (say) is evaluated as,

$$
\begin{aligned}
&\boldsymbol{r}_{CP_j} = \left[T_{\beta}^{\boldsymbol{r}_{B_j}}\right] \left[T_{\alpha_3}^{\boldsymbol{n}_{P_i}}\right] \boldsymbol{r}_{B_j} \\
&\text{where} \quad \boldsymbol{n}_{P_j} = \frac{\boldsymbol{r}_{B_j} \times \boldsymbol{r}_{C_j}}{||\boldsymbol{r}_{B_j} \times \boldsymbol{r}_{C_j}||} \\
&\text{for} \quad j = 1, 2, \ldots, 100
\end{aligned}
\tag{28}
$$

For the i^{th} coupler path, let P_k^i, $\boldsymbol{r}_{P_k}^i$ be the given k^{th} data point. The error in k^{th} data point is given by,

$$
\begin{aligned}
&e_k^i = \min\left\{e_{k1}^i, e_{k2}^i, \ldots, e_{kj}^i, \ldots, e_{k100}^i\right\} \\
&e_{kj}^i = ||\boldsymbol{r}_{CP_j}^i - \boldsymbol{r}_{P_k}^i||, \quad j = 1, 2, \ldots, 100, \quad k = 1, 2, \ldots, N_r, \quad i = 1, 2, \ldots, m
\end{aligned}
\tag{29}
$$

where N_r is the number of data-points given initially representing each coupler path and m is the number of coupler paths to be traced. The maximum error and the total error for the i^{th} coupler path is given as,

$$
\begin{aligned}
E_{max}^i &= \max\left\{e_1^i, e_2^i, \ldots, e_k^i, \ldots, e_{N_r}^i\right\} \\
E_{path}^i &= \sum_{k=1}^{N_r} e_k^i
\end{aligned}
\tag{30}
$$

The total error for all the m coupler paths is given by,

$$
E_{Total} = \sum_{i=1}^{m} E_{path}^i \tag{31}
$$

If the adjustment cannot be chosen by $(S + f)_{min}$, then E_{Total} must be evaluated for each adjustment type after obtaining all the optimal mechanism parameters. The adjustment type with minimum E_{Total} must be chosen.

The steps in the optimal synthesis of an adjustable spherical mechanism for multi-path generation is shown in the flowchart given in figure 3. In the next section we present examples which illustrates the developed approach.

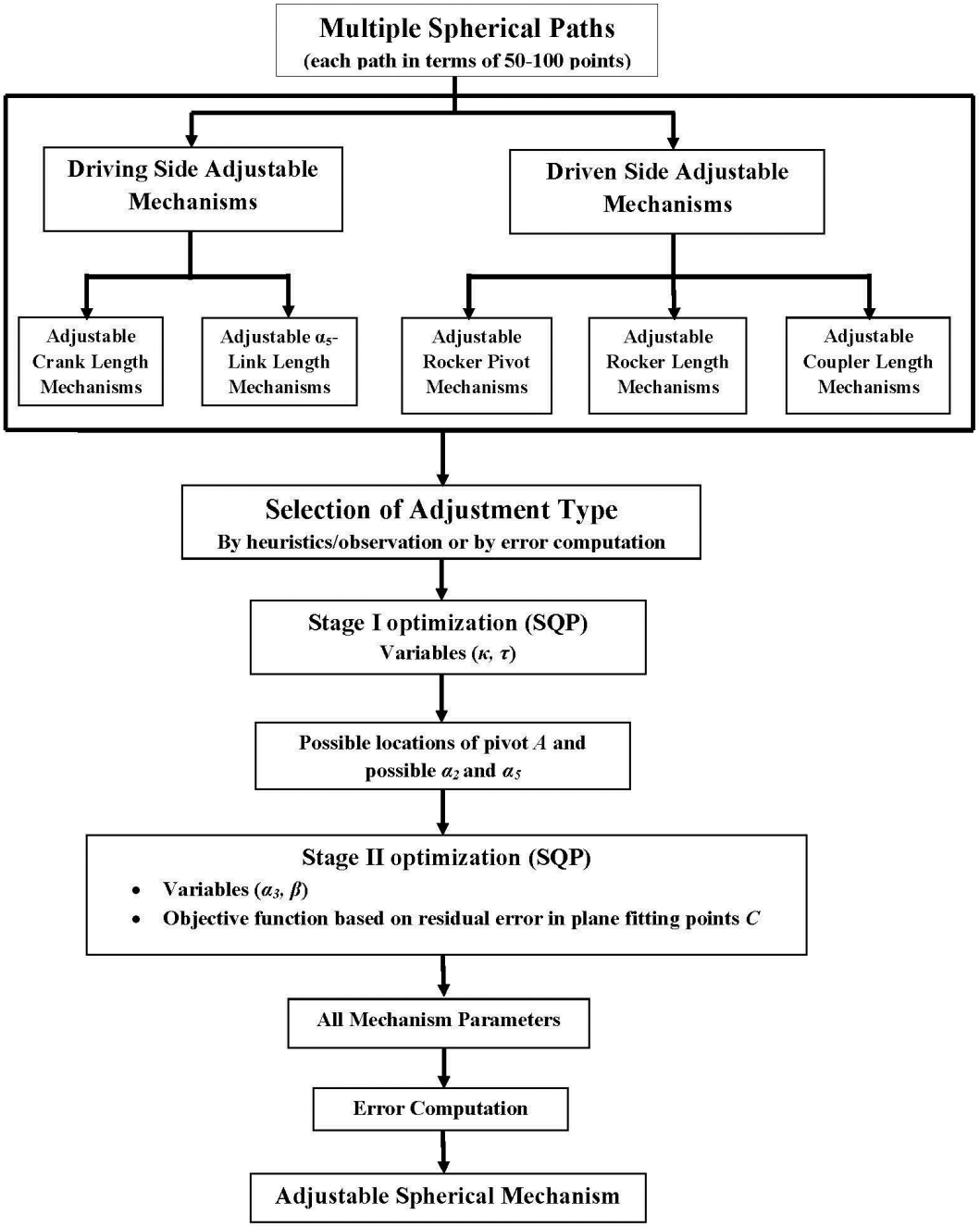

Figure 3: Flowchart of the synthesis process

4 Results and discussion

To demonstrate the use of the proposed methodologies we present two examples, one for an adjustable driving side mechanism and one for an adjustable driven side mechanism. Simulations were done using 64-bit Matlab [38], version R2011b on a PC with Intel Core-2-Quad 2.4 GHz processor and 4 GB of RAM. The optimization was done using 'fmincon' function of Matlab.

4.1 Example 1

The first example presented is for synthesis of adjustable crank length mechanism. The data points are taken on the XY-plane and then projected on the sphere $x^2 + y^2 + z^2 = 1$. The qualitative behaviour of coupler paths with change in crank length has been taken into account. The two elliptical paths on XY-plane are represented by,

$$\text{Path } 1 = (1 + 0.25\cos t, 0.02 + 0.15\sin t)$$
$$\text{Path } 2 = (1 + 0.4\cos t, 0.22\sin t)\,, \quad t \in [0, 2\pi]$$

The points inside the circle $x^2 + y^2 = 1$ in the XY-plane are used to generate the spherical path as shown in Figure 4a. These points are projected on both the hemispheres of the sphere $x^2 + y^2 + z^2 = 1$. A total 46 data points are taken on each path. The optimization results are as follows:

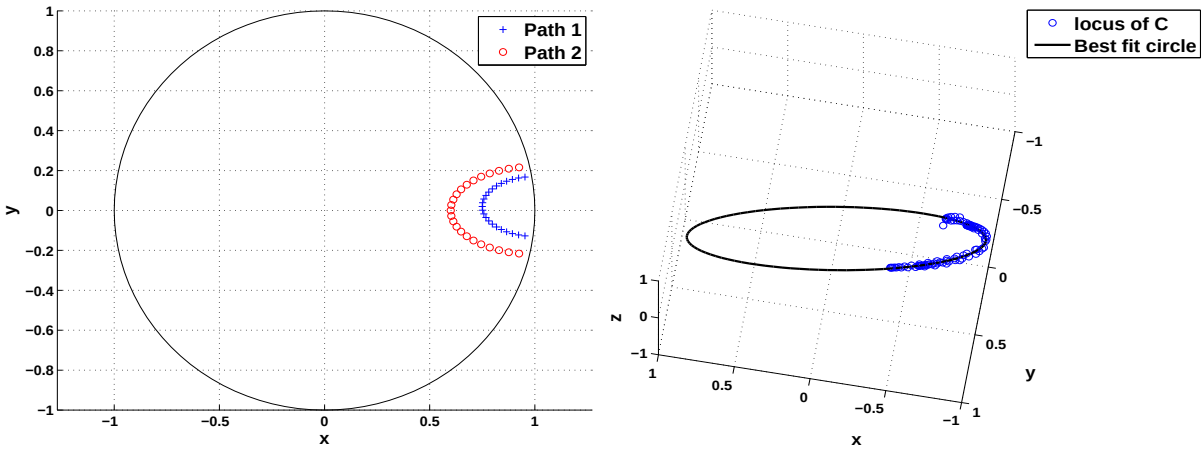

(a) Desired paths in XY-plane

(b) Locus of C

Figure 4: Example 1

Stage I optimization
The search space, $\kappa \in [0, \pi]$ is divided into 5 intervals and $\tau \in [0, 2\pi]$ is divided into 10 intervals. From the approach described in section 3, S_{max} is chosen to be 10^{-6} which results in 36 possible dyads.
Stage II optimization
In this case, $\alpha_3 \in [0.9 \text{ rad}, \pi]$ is divided into 3 intervals and $\beta \in [-\pi, \pi]$ is divided in 4 intervals. The results of the optimization and values of selected mechanism parameters are as follows:
Value of the cost function, $S = 10^{-7}$.
$\kappa = 2.5133$ rad, $\tau = 0.0066$ rad, Coordinates of $A = (0.5878, 0.0038, -0.8090)$, $\alpha_2^1 = 0.7222$ rad,

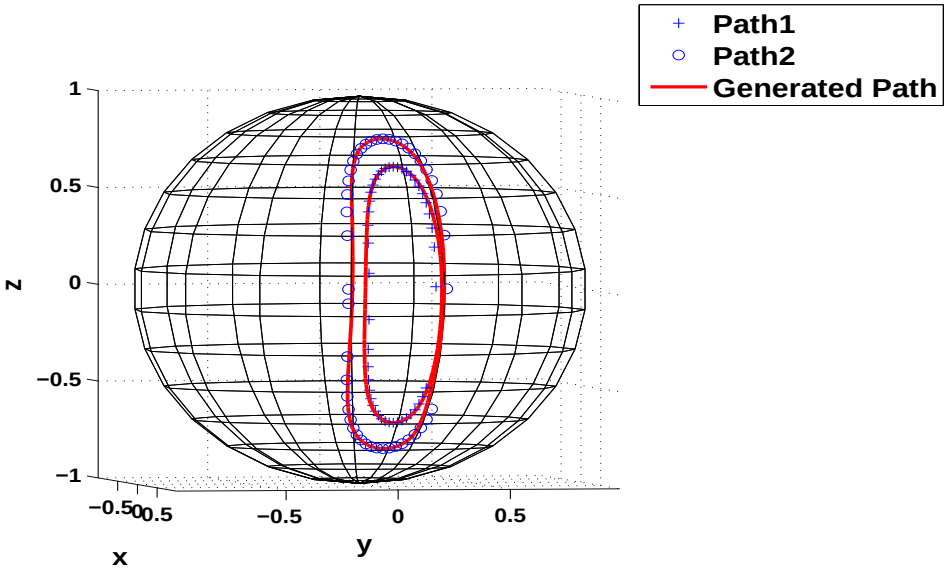

Figure 5: Example 1 – Generated and desired paths

$\alpha_2^2 = 0.9271$ rad, $\alpha_5 = 0.9427$ rad.
$f = 0.0150$, $\alpha_1 = 1.6381$ rad, $\alpha_3 = 1.9518$ rad, $\alpha_4 = 1.3367$ rad, $\beta = 2.9961$ rad, and Coordinates of $D = (-0.1635, 0.9861, -0.0310)$.
The optimal spatial circle for rocker point C is shown in Figure 4b and the generated and desired paths are shown in Figure 5. The maximum error for each path are:
Path 1, $E_{max} = 0.0280$, and
Path 2, $E_{max} = 0.0379$.

4.2 Example 2

In the second example, we present the synthesis, kinematic design, prototype manufacturing and testing of a driving mechanism for a planned flapping wing micro air vehicle. The goal for the synthesized mechanism is to mimic the wing-tip path for a bird in flight. It is known from literature [39, 40, 41, 42] that to generate lift, the orientation of the wing of a bird is such that the wing-tip makes a '8' shaped path when the bird is hovering and an oval shaped path when the bird is in forward flight. This example uses the qualitative nature of the wing-tip paths given in the above references to synthesize an adjustable 4R spherical mechanism whose coupler point can generate the two mentioned paths. The '8' shaped path is bi-symmetrical and is generated by reflecting the half lobe of the '8' path shown in Figure 6a on the hemisphere across the XZ-plane. The '8' shaped path is generated using the atlas given in reference [19]. The second oval path is generated by increasing the base angle of the same mechanism to 60 degrees.
We follow the two stage optimization presented in this work and the optimization results are as follows:
Stage I optimization
The search space, $\kappa \in [0, \pi]$ is divided into 5 intervals and $\tau \in [0, 2\pi]$ is divided into 10 intervals. Following the approach in section 3, S_{max} is chosen to be 10^{-5} which results in 10 possible dyads.
Stage II optimization
In this case, $\alpha_3 \in [0.6 \text{ rad}, 2.5 \text{ rad}]$ is divided into 4 intervals and $\beta \in [-\pi, \pi]$ is divided in 4 intervals. The results of the optimization and the parameters of the selected mechanism are as follows:

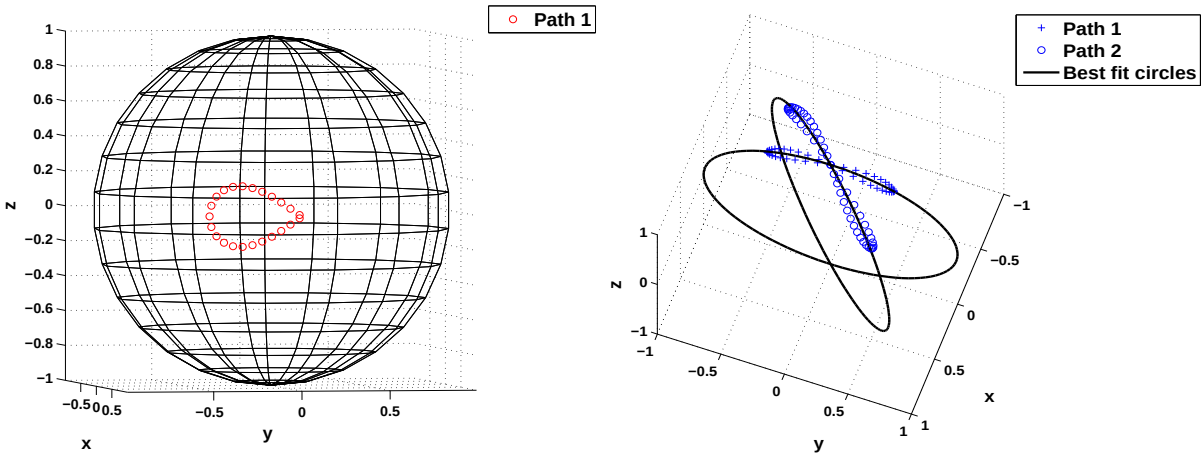

(a) Half-lobe of '8' path

(b) Locus of C for '8' and oval paths

Figure 6: Example 2

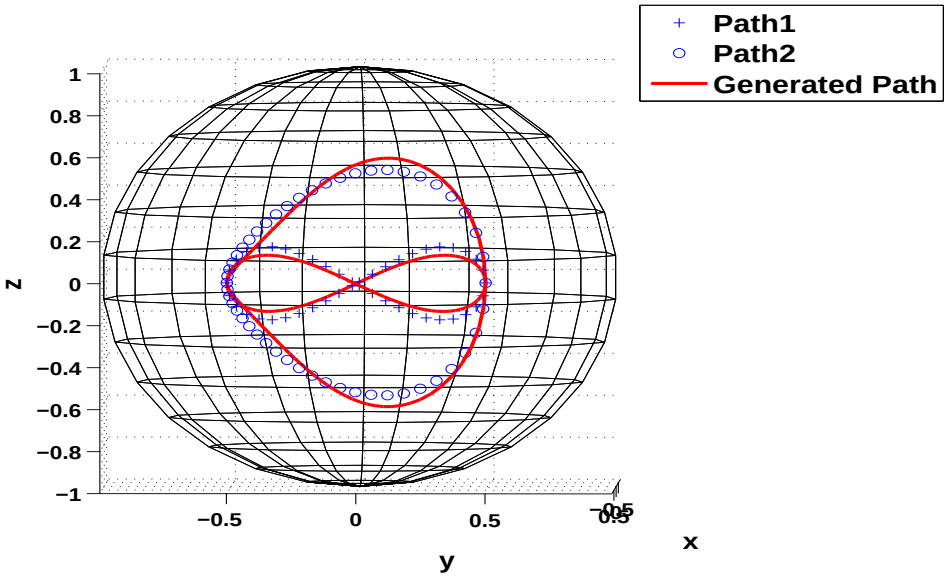

Figure 7: Example 2 – Generated and desired paths

Value of the cost function, $S = 10^{-7}$.
$\kappa = 1.5708$ rad, $\tau = 1.5708$ rad, Coordinates of $A = (0, 1, 0)$, $\alpha_2 = 0.5236$ rad, and $\alpha_5 = 1.5708$ rad. $f = 0.0787$, $\alpha_1^1 = 1.5708$ rad, $\alpha_1^2 = 0.7982$ rad, $\alpha_3 = 1.5708$ rad, $\alpha_4 = 1.5708$ rad, $\beta = 1.5708$ rad, Coordinates of $D_1 = (-1, 0, 0)$ and $D_2 = (-0.7161, 0.6980, 0)$.
The optimal spatial circle for rocker point C is shown in figure 6b. The generated and desired paths are shown in figure 7.

A prototype of the spherical mechanism, with the parameters obtained from optimization as mentioned above, was manufactured using 3D printing technique and was tested for the generation of the '8' and oval shaped coupler paths. The mechanism is expected to generate the figure of

'8' shape when the base link α_1 is 1.5708 rad and the oval shape path when the base link α_1 is 0.7982 rad. The CAD model of the mechanism in the two configurations is shown in figure 8. The

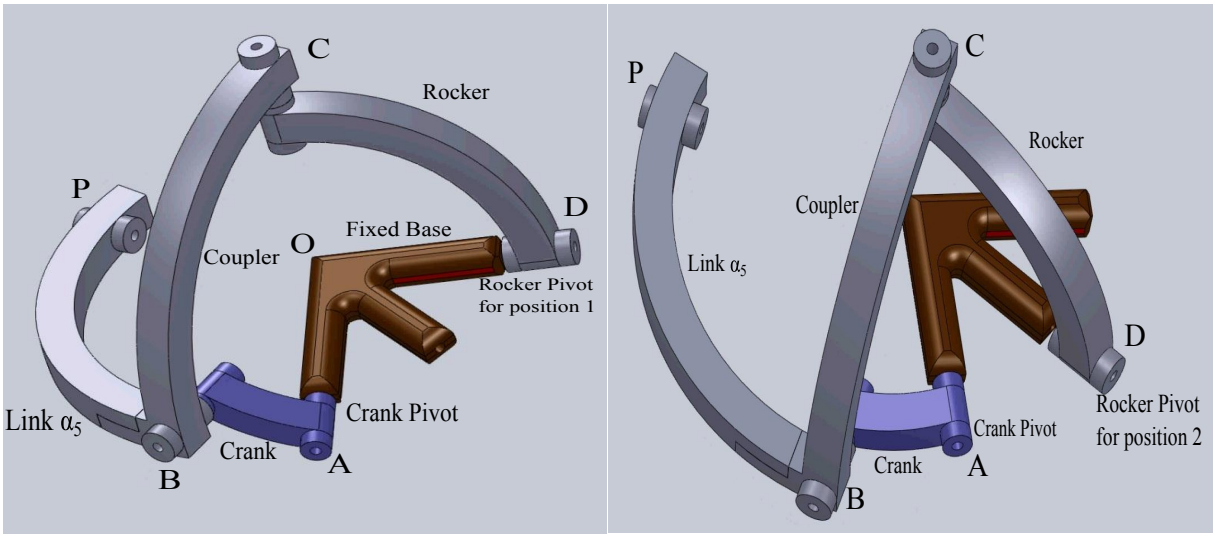

(a) Figure '8' position

(b) Oval shape position

Figure 8: CAD model of adjustable spherical 4R mechanism

manufactured prototype is shown in figure 9. The wing is attached at the coupler point P and other various links as well as the adjustment parameter are marked in figure 9. The adjustment is done using a small stepper motor placed at the center of the sphere and as the stepper motor rotates the base link OD gradually, the position of the rocker pivot D changes. The driving motor and the small stepper motor can be remotely controlled. As the stepper motor changes the location of the pivot D, one can observe that the coupler path changes from an '8' shape to an oval shape and vice-versa. These transformations can be seen in the attached video where the path traced is shown with a light emitting diode (LED). In an actual flapping wing micro air vehicle, a solenoid can be used for achieveing the two positions of the rocker pivot D and only one driving motor will be required. This work is continuing and we are attempting to make the flapping wing micro air vehicle exhibit forward and hovering motion using the adjustment mechanism presented in this example.

5 Conclusion

This paper presents a novel optimization based methodology for synthesising adjustable spherical four-link mechanisms for approximate multi-path generation. The adjustments are made in the five different parameters of the mechanism. The objective functions used in the optimization process for obtaining the various parameters uses the least possible number of variables – in the most common type of adjustments, only two parameters in each of the two stages, namely the crank and coupler length adjustment for the driving side and rocker-link and rocker-link fixed pivot adjustment of the driven side, are involved. The method uses a modified least-squares based plane fitting technique and is found to be very efficient. Various constraints are suggested to sort the appropriate mechanism and the method does not require a starting point to be given by the user for the SQP optimization. The method presented in this work is also capable of synthesizing adjustable mechanism for more than two paths. The kinematic design of a practical adjustable mechanism for a flapping wing micro air vehicle, capable of forward and hovering motion, has been designed, manufactured and tested and the method proposed in this work appears to yield satisfactory results.

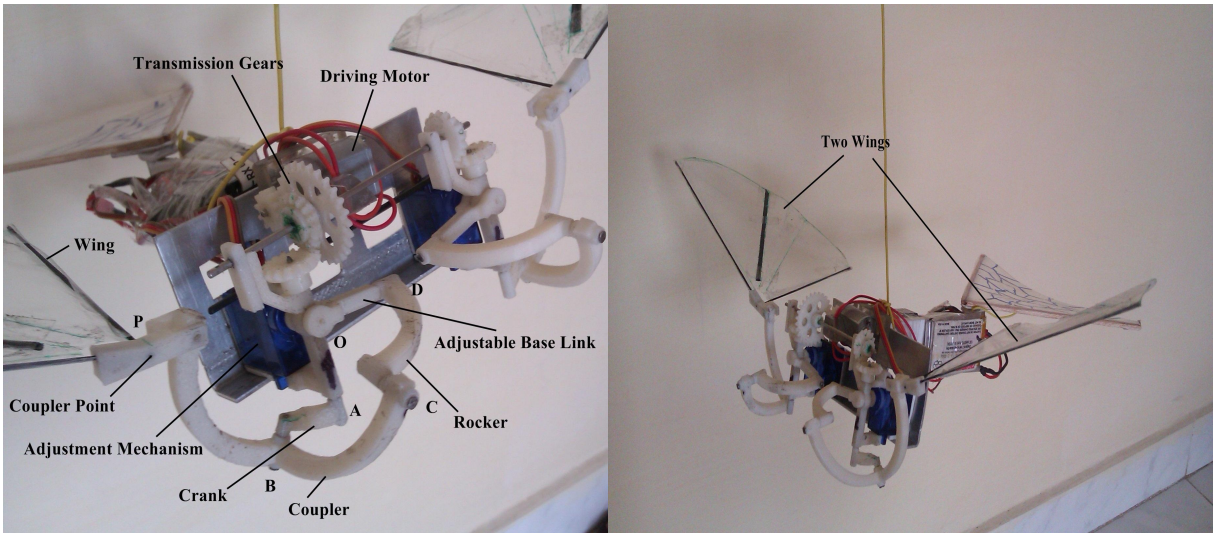

(a) Driving 4R spherical mechanism (b) Prototype of flapping wing micro air vehicle

Figure 9: Manufactured prototype

References

[1] C. H. Chiang, *Kinematics of Spherical Mechanisms*, Cambridge University Press, Cambridge, 1988.

[2] J. J. Uicker, G. R. Pennock and J. E. Shigley, *Theory of Machines and Mechanisms*, Oxford University Press, New York, 2005.

[3] D. Chabalat and J. Angeles, 'The computation of all 4R spherical serial spherical wrists with an isotropic architecture', *Trans. ASME, Journal of Mechanical Design*, Vol. 125, No. 2, pp. 275-280, June 2003.

[4] M. J. H. Lum, J. Rosen, M. N. Sinanan and B. Hannaford, 'Optimization of a spherical mechanism for a minimally invasive surgical robot: theoretical and experimental approaches', *IEEE Transactions on Biomedical Engineering*, Vol. 53, No. 7, pp. 1440-1445, July 2006.

[5] M. McDonald and S. K. Agrawal, 'Design of a bio-inspired spherical four-bar mechanism for flapping-wing micro air-vehicle applications', *Trans. ASME, Journal of Mechanisms and Robotics*, Vol. 2, No. 2, pp. 1-6, May 2010.

[6] H. Kocabas, 'Gripper design with spherical parallelogram mechanism', *Trans. ASME, Journal of Mechanical Design*, Vol. 131, No. 7, pp. 1-9, July 2009.

[7] J. S. Ketchel and P. M. Larochelle, 'Computer-aided manufacturing of spherical mechanisms', *Mechanism and Machine Theory*, Vol. 42, pp. 131-146, 2007.

[8] C. M. Gosselin and J. -F. Hamel, 'The agile eye: a high performance three-degree-of-freedom camera-orienting device', *IEEE Conference on Robotica and Automation*, San Diego, pp. 781-787, 1994.

[9] C. Menon, R. Vertechy, M. C. Markót and V. Parenti-Castelli, 'Geometrical optimization of parallel mechanisms based on natural frequency evaluation: application to a spherical mechanism for future space applications', *IEEE Transactions on Robotics*, Vol. 25, No. 1, pp. 12-24, 2009.

[10] R. V. Dukkipati, *Spatial Mechanisms: Analysis and Synthesis*, Narosa Publishing House, New Delhi, 2001.

[11] Z. Liu, *Optimization of Spherical Four-Bar Path Generators*, M. Eng. Thesis, McGill University, Montréal, November 1988.

[12] R. S. Sodhi and T. E. Shoup, 'Axodes of the four revolute spherical mechanisms', *Mechanism and Machine Theory*, Vol. 17, pp. 173-178, 1982.

[13] R. S. Sodhi, A. J. Wilhelm and T. E. Shoup, 'Design for a four revolute spherical function generator with transmission effectiveness by curve matching', *Mechanism and Machine Theory*, Vol. 20, pp. 577-585, 1985.

[14] S. -H. Tong and C. H. Chiang, 'Synthesis of planar and spherical four-bar path generators by the pole method', *Mechanism and Machine Theory*, Vol. 27, pp. 145-155, 1992.

[15] R. M. C. Bodduluri and J. M. McCarthy, 'Finite position synthesis using the image curve of a spherical four-bar motion', *Trans. ASME, Journal of Mechanical Design*, Vol. 114, No. 1, pp. 55-60, 1992.

[16] D. A. Ruth and J. M. McCarthy, 'The design of spherical 4R linkages for four specified orientations', *Mechanism and Machine Theory*, Vol. 34, pp. 677-692, 1999.

[17] C. -C. Lin, 'Complete solution of the five-position synthesis for spherical four-bar mechanisms', *Journal of Marine Science and Technology*, Vol. 6, No. 1, pp. 17-27, 1998.

[18] J. Angeles and Z. Liu, 'The constrained least-square optimization of spherical four-bar path generators', *Trans. ASME, Journal of Mechanical Design*, Vol. 114, No. 3, pp. 394-405, 1992.

[19] D. -M. Lu, 'A triangular nomogram for spherical symmetric coupler curves and its applications to mechanical design', *Trans. ASME, Journal of Mechanical Design*, Vol. 121, No. 2, pp. 323-326, 1999.

[20] J. Chu, J. Sun, 'Numerical atlas method for generation of spherical four-bar mechanism', *Mechanism and Machine Theory*, Vol. 45, pp. 867-879, 2010.

[21] G. Mullineux, 'Atlas for spherical four-bar mechanisms', *Mechanism and Machine Theory*, Vol. 46, pp. 1811-1823, 2011.

[22] F. Peñuñuri, R. Peón-Escalante, C. Villanueva and C. A. Cruz-Villar, 'Synthesis of spherical 4R mechanism for path generation using differential evolution', *Mechanism and Machine Theory*, Vol. 57, pp. 62-70, 2012.

[23] Y. -F. Liu and S. -X. Yang 'Advances and trends in spherical mechanisms and research', *Machine Design and Research*, Vol. 26, No. 1, pp. 32-35, 2010.

[24] W. -T. Lee, *The Design of Adjustable Spherical Mechanisms using Plane-to-sphere and Sphere-to-plane Projections*, Ph. D Dissertation, New Jersey Institute of Technology, New Jersey, 2004.

[25] B. Hong and A. G. Erdman, 'A method for adjustable planar and spherical four-bar linkage synthesis', *Trans. ASME, Journal of Mechanical Design*, Vol. 127, No. 3, pp. 456-463, 2005.

[26] W. -T. Lee, K. Russell, Q. Shen and R. S. Sodhi, 'On adjustable spherical four-bar motion generation for expanded prescribed positions', *Mechanism and Machine Theory*, Vol. 44, pp. 247-254, 2009.

[27] H. Funabashi, N. Iwatsuki and Y. Yokoyama, 'A synthesis of crank-length adjusting mechanisms', *Bulletin of Japan Society of Mechanical Engineers*, Vol. 29, No. 252, pp. 1946-1951, 1986.

[28] Z. Junfu, X. Liju and W. Jinge, 'Path synthesis of adjustable spherical four-bar mechanisms based on chaos fractal algorithm', *Mechanical Science and Technology*, Vol. 26, Part 2, pp. 172-176, 2007.

[29] Chong Peng and R. S. Sodhi, 'Optimal synthesis of adjustable mechanisms generating multiphase approximate paths', *Mechanism and Machine Theory*, Vol. 45, pp. 989-996, 2010.

[30] J. S. Arora, *Introduction to Optimum Design*, Academic Press, New Delhi, 2012.

[31] P. V. Chanekar and A. Ghosal, 'Optimal synthesis of adjustable planar four-bar crank-rocker type mechanisms for approximate multi-path generation', *Mechanism and Machine Theory*, Vol. 69, pp. 263-277, 2013.

[32] A. Ghosal, *Robotics: Fundamental Concepts and Analysis*, Oxford University Press, New Delhi, 2006.

[33] W. Gander, G. H. Golub and R. Strebel, 'Least-squares fitting of circles and ellipses', *BIT Numerical Mathematics*, Vol.34, No. 4, pp. 558-578, 1994.

[34] P. E. Gill, W. Murray and M. H. Wright, *Practical Optimization*, Academic Press, New York, 1981.

[35] J. A. Hrones and G. L. Nelson, *Analysis of the Four-bar Linkage*, The Technology Press of M.I.T. and John Wiley & Sons, Inc., New York, 1951.

[36] A. Guha and C. Amarnath, 'Adjustable mechanism for walking robots with minimum number of actuators', *Chinese Journal of Mechanical Engineering*, Vol. 24, No. 5, pp. 760-767, 2011.

[37] J. J. Cervantes-Sánchez, H. I. Medellín, J. M. Rico-Martínez, E. J. González-Galván, 'Some improvements on the exact kinematic synthesis of spherical 4R function generators', *Mechanism and Machine Theory*, Vol. 44, pp. 103-131, 2009.

[38] MATLAB, *Version 7.12.0 (R2011a)*, The MathWorks Inc., Natick, Massachusetts, 2012.

[39] W. Shyy, Y. Lian, J. Tang, D. Viieru and H. Liu, *Aerodynamics of Low Reynolds Number Flyers*, Cambridge University Press, New York, 2008.

[40] G. Bunget, *BATMAV: A Biologically-Inspired Micro-Air Vehicle for Flapping Flight-Kinematic Modeling*, M. S. Thesis, North Carolina State University, Raleigh, 2007.

[41] R. L. Harmon, *Aerodynamic Modeling of a Flapping Membrane Wing using Motion Tracking Experiments*, M. S. Thesis, University of Maryland, College Park, 2008.

[42] Michael A A. Fenelon, 'Biomimetic flapping wing aerial vehicle', *IEEE International Conference on Robotics and Biomimetics*, pp. 1053-1058, 2008.

List of Figure Captions

Figure 1: Schematic of a spherical 4R mechanism
Figure 2: Crank angle and a spherical dyad
Figure 3: Flowchart of the synthesis process
Figure 4: Example 1
Figure 5: Example 1 – Generated and desired paths
Figure 6: Example 2
Figure 7: Example 2 – Generated and desired paths
Figure 8: CAD model of adjustable spherical 4R mechanism
Figure 9: Manufactured prototype

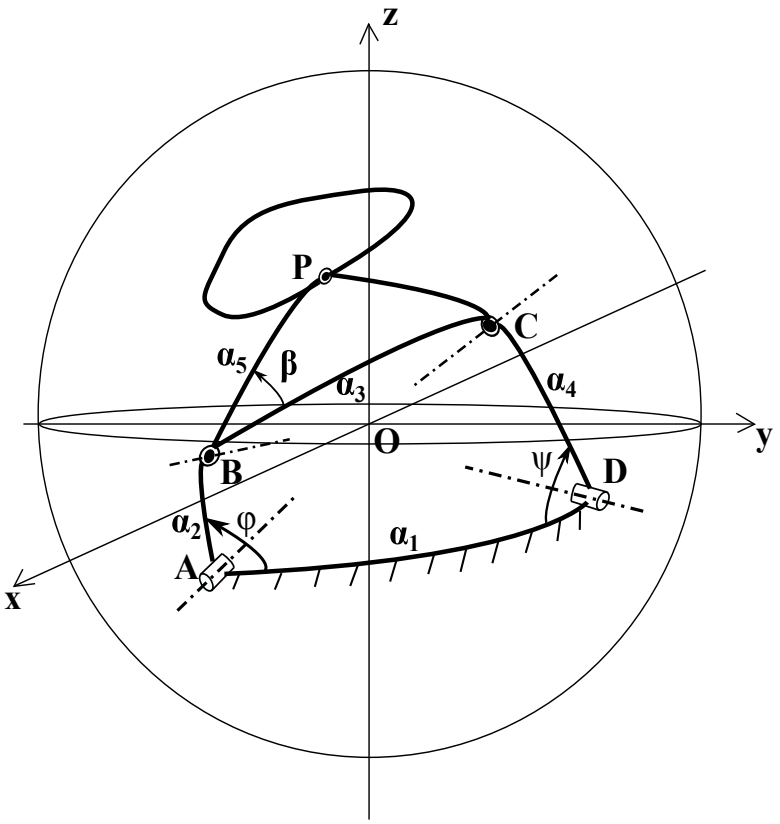

Figure 1: Schematic of a spherical 4R mechanism

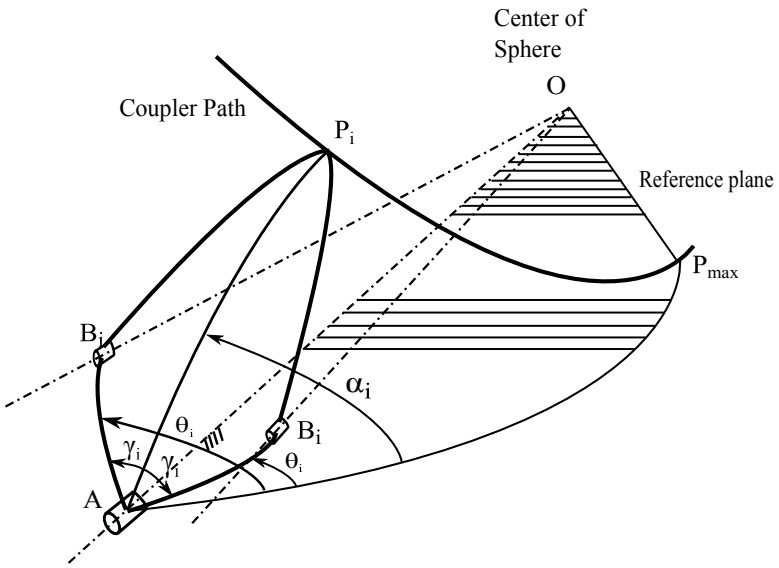

Figure 2: Crank angle and a spherical dyad

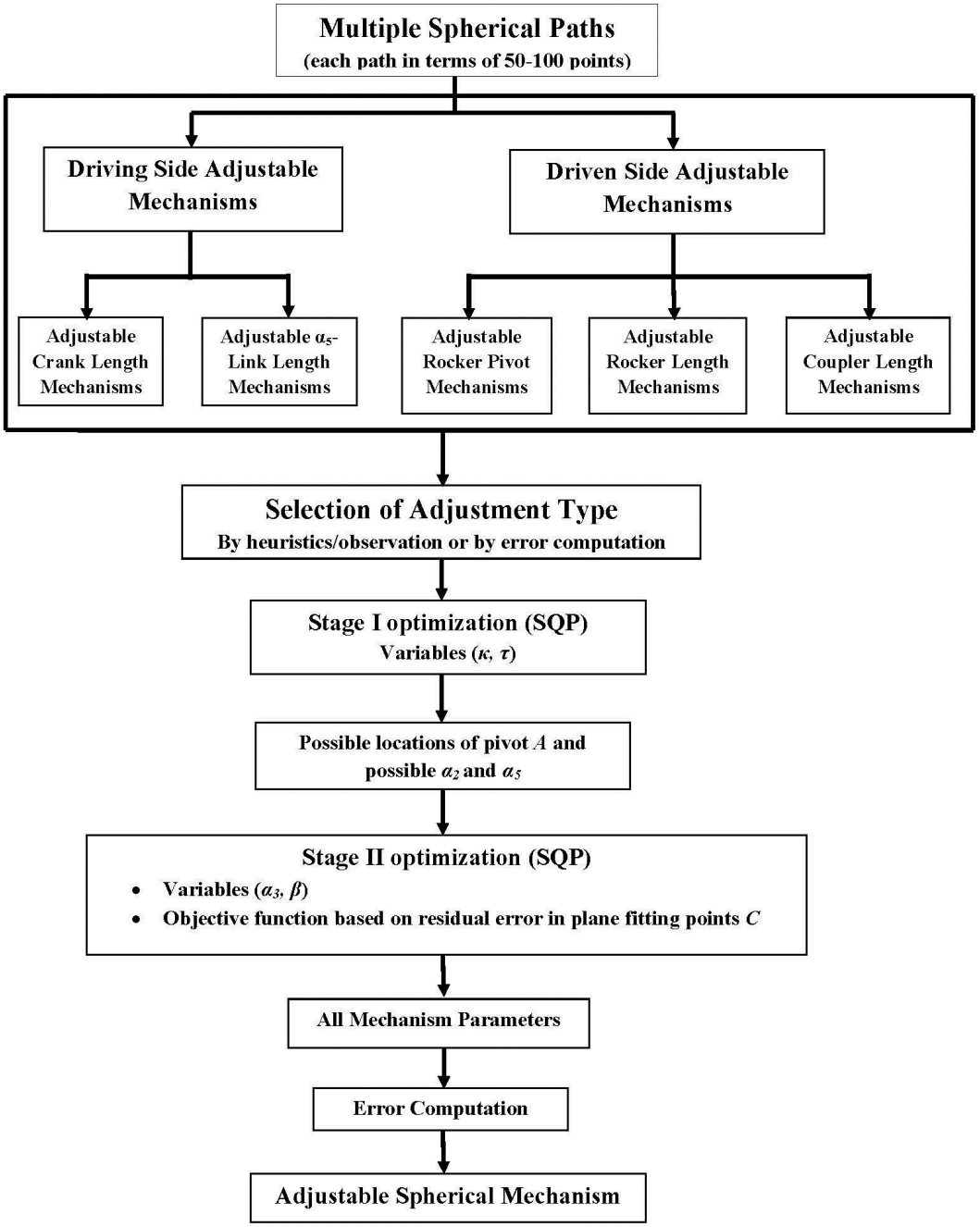

Figure 3: Flowchart of the synthesis process

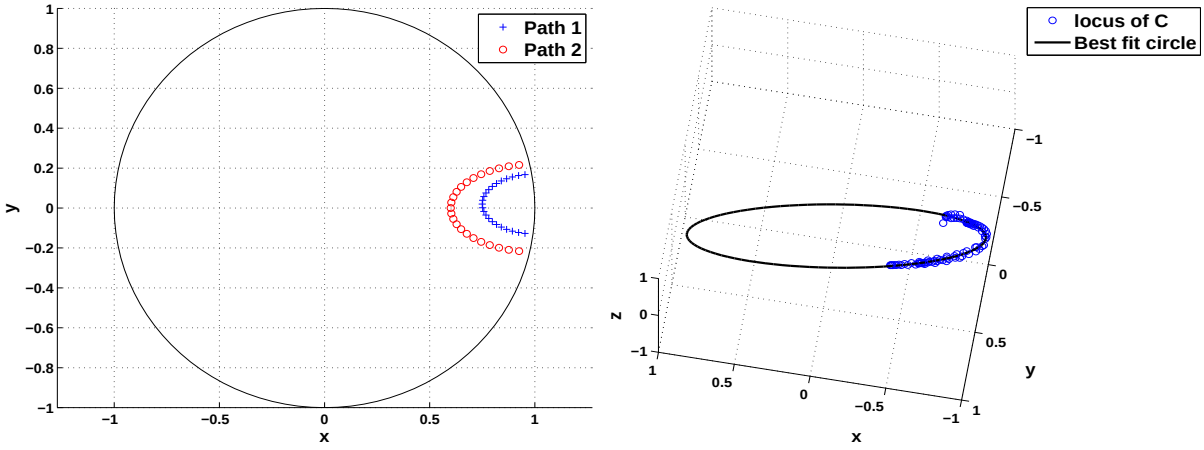

(a) Desired paths in XY-plane

(b) Locus of C

Figure 4: Example 1

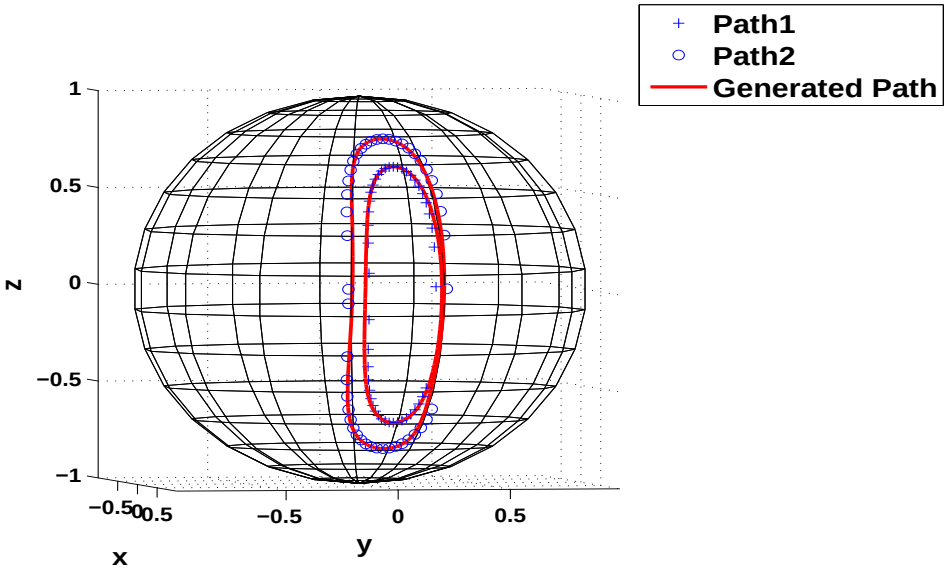

Figure 5: Example 1 – Generated and desired paths

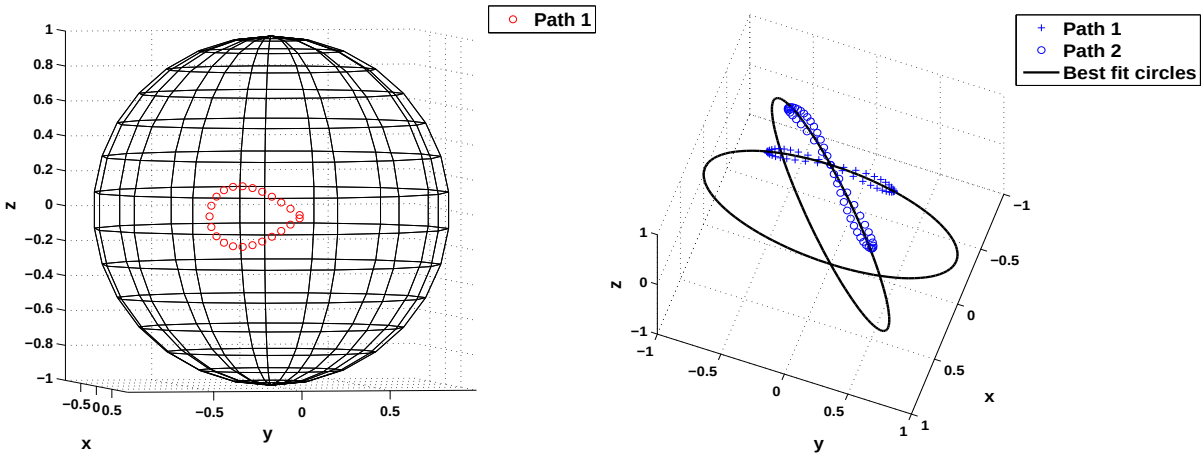

(a) Half-lobe of '8' path

(b) Locus of C for '8' and oval paths

Figure 6: Example 2

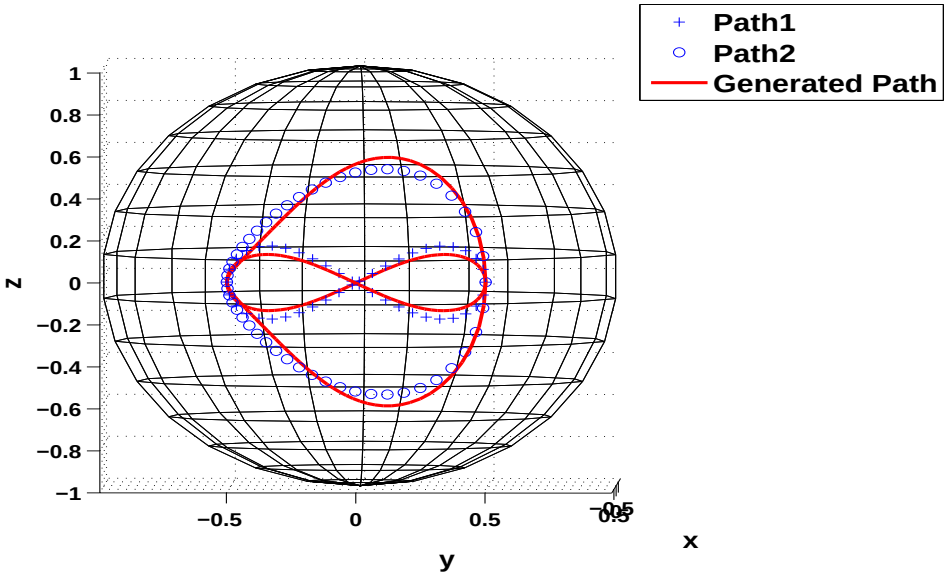

Figure 7: Example 2 – Generated and desired paths

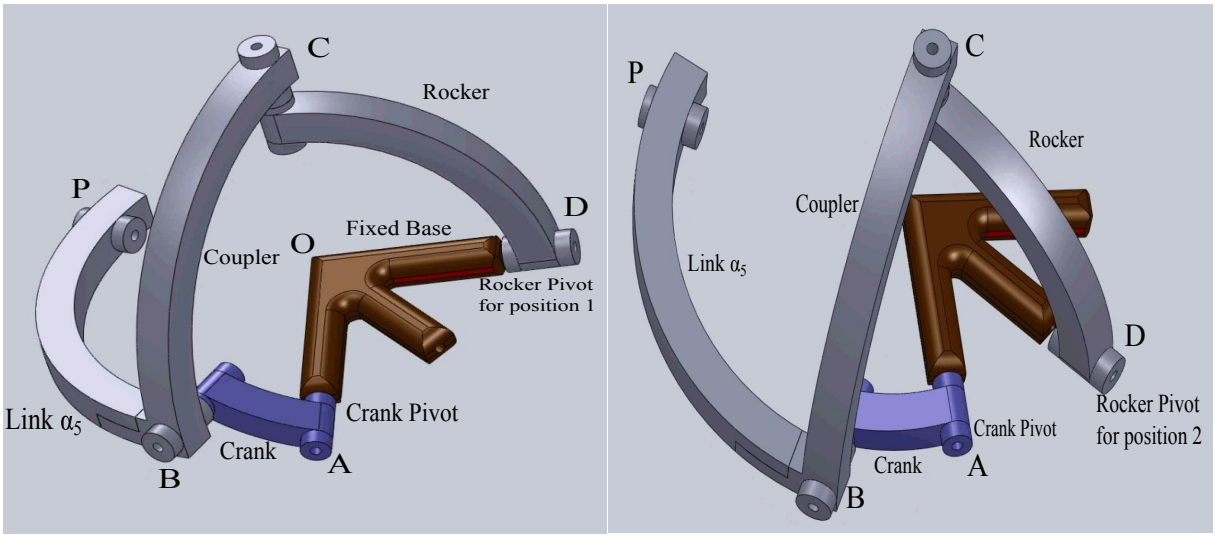

(a) Figure '8' position

(b) Oval shape position

Figure 8: CAD model of adjustable spherical 4R mechanism

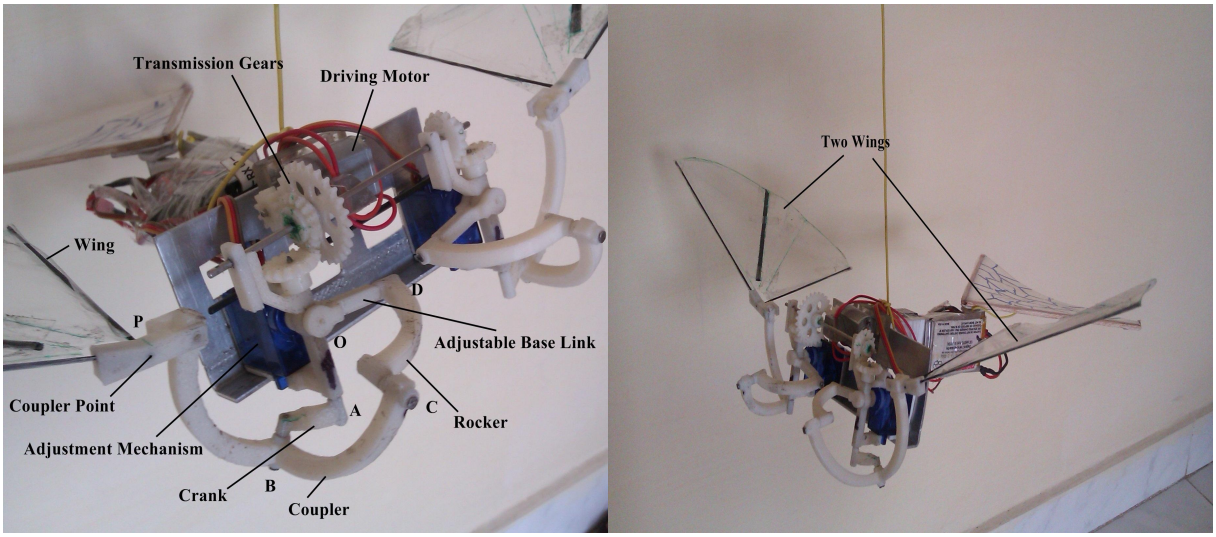

(a) Driving 4R spherical mechanism (b) Prototype of flapping wing micro air vehicle

Figure 9: Manufactured prototype